International Refrigeration and Air Conditioning Conference

School of Mechanical Engineering

2010

Electrical Determination of Reciprocating Compressor Instantaneous Angular Speed

Christopher Schantz
MIT Labratory for Electromagnetic and Electronic Systems

Zack Remscrim
MIT Labratory for Electromagnetic and Electronic Systems

Steven B. Leeb
MIT Labratory for Electromagnetic and Electronic Systems

Follow this and additional works at: http://docs.lib.purdue.edu/iracc

Schantz, Christopher; Remscrim, Zack; and Leeb, Steven B., "Electrical Determination of Reciprocating Compressor Instantaneous Angular Speed" (2010). *International Refrigeration and Air Conditioning Conference.* Paper 1136.
http://docs.lib.purdue.edu/iracc/1136

Electrical Determination of Reciprocating Compressor Instantaneous Angular Speed

Christopher Schantz[1]*, Zack Remscrim[2], Steven Leeb[3]

[1,2,3] Massachusetts Institute of Technology, Research Laboratory for Electronics;
Laboratory for Electromagnetic and Electronic Systems, Cambridge, MA, USA
[1] cschantz@mit.edu, [2] remscrim@mit.edu, [3] sbleeb@mit.edu

* Corresponding Author

ABSTRACT

HVAC compressor units are major energy consumers in both residential and commercial buildings today. Faulty and energy wasting operation of these units often goes unnoticed due to the corrective action of feedback control. Power system monitoring is an exciting approach for creating inexpensive, highly capable methods to monitor compressor unit performance. In this paper we develop a method to estimate the instantaneous angular speed (IAS) of the shaft of a reciprocating compressor from the drive motor's electric signals. Solving the dynamic model of the induction motor overcomes the difficulties that other speed estimation algorithms encounter when the mechanical dynamics are on the same time scale as the electrical dynamics. This procedure obtains useful diagnostic information internal to the compressor without the difficulty of mechanical sensor installation.

1. INTRODUCTION

Reciprocating compressors are widely used in many industries, from chemical and process plants to refrigeration and thermal comfort applications. They comprise an essential component in many vapor compression air conditioners or heat pumps, and these devices are widely present in HVAC systems. As opposed to compressors in the chemical and process industries, the operation of compressors in HVAC units is usually hidden from the user. This lack of awareness of the detailed operation of the HVAC system combined with standard feedback control strategies gives rise to situations where unhealthy or faulty operation of the compressor can go unnoticed for long periods of time. Feedback control will tend to operate the faulty compressor system at an ever increasing duty cycle to maintain the set point as the unit gradually degrades and the greater run time will waste large amounts of energy as well as cause undue wear on the other components of the system. The fault is usually noticed, if ever, only when the system has degraded so severely that continuous operation is insufficient to maintain the user's desired set point.

Power system monitoring is an exciting approach for creating inexpensive and highly capable algorithms to monitor the health of systems like the above under the operation of feedback control. The large majority of compressors are driven by electric motors, with three phase induction motors being arguably the most common. This work focuses on the derivation of an estimate of IAS of an induction motor driven a reciprocating compressor using electrical measurements and knowledge of machine parameters. The method is not limited to reciprocating compressors, as it should apply to any induction motor driven machine. Unlike past speed sensorless speed detection algorithms (Kim *et al.* 1994) developed for high performance servo motor control applications, such as extended Kalman filters (Shi *et al.* 2002) or observers, the method is able to very accurately account for the minor speed variations over the course of a single shaft rotation in sufficient detail to open a window on the dynamics and health of the driven load.

The IAS has been shown to be an effective tool in detecting various faults in a reciprocating compressor. Al-Qattan *et al.* (2009), listed a source that was able to detect valve faults using the deviations of the IAS of a reciprocating compressor form a baseline IAS and the relative angles at which the deviations occurred. Al-Qattan *et al.* (2009) presented a simulation study showing the effect of suction and discharge valve faults, suction pressure variation, and excess clearance faults in the compressor cylinder on a double acting single cylinder hydrogen make up compressor's IAS and instantaneous power consumption. A numerical simulation by Elhaj *et al.* (2008) of a two stage belt driven reciprocating compressor has also shown that both the IAS fluctuations and the cylinder pressure waveform are sensitive to valve leakage and other faults. In this study the IAS is preferred because of the much less intrusive nature of installing a speed sensor versus installing cylinder pressure sensors. Angrilli and Basso (1994) investigated stress monitoring in a reciprocating mechanism in applications involving cutting machinery and found

value in the IAS and instantaneous motor torque. There is also a body of similar work on internal combustion engines see Jacob *et al.* (1999), Gu *et al.* (1999), or Citron et al. (1989) for example.

To our knowledge all previous work in this vein has relied on either simulation or the explicit instillation of a speed sensor such as a shaft encoder, DC motor tachometer, or a magnetic gear tooth counter. Since these sensors (especially the magnetic gear tooth counter) do not involve extensive modifications to the machine, some authors have taken to calling speed measurement in this fashion "non-intrusive." In comparison our method relies purely on electrical measurements, with sensor installation as simple as plugging a machine into a standard wall outlet, and is therefore much more non-intrusive. In fact, our experimental validation involves the IAS sensing of a semi-hermetically sealed reciprocating compressor where installation of a speed sensor without compromising the pressure vessel is practically impossible in a field or maintenance setting. Our technique allows the compressor's induction motor to become its own speed and torque sensor.

2. INSTURMENTATION AND EXPERIMENTAL METHOD

The compressor studied is a KAMA-007A-TAC-800 compressor modified with high dynamic range in-cylinder pressure sensors and a 2500 count shaft encoder. The compressor shaft was made accessible via a custom shaft extension brought through a machined hole in the compressor case. The voltage and current signatures are measured on all three phase of the machine via LV-25P voltage transducers and LA-55 current transducers. The electrical instrumentation was developed in the LEES lab as part of the non-intrusive load monitor concept over a number of years (Shaw et al. 2008). All instruments are read via a data acquisition card at a high data rate of 7 kHz or greater depending on the number of simultaneous channels. The encoder pulse train was divided via a counter chip by a factor of 32 to increase the resolution of the speed reading in the range of interest (1800 rpm). The data acquisition card's on board 48 MHz clock is used to count elapsed time between the successive encoder pulses (after division). A National Instruments EDAC2 is fed the raw encoder pulse train to record the angular position of the compressor shaft. The shaft encoder was mounted on its own precision shaft running between dedicated bearing blocks to ensure no eccentric motion of the encoder case which would result in false speed readings. This dedicated shaft was connected to the shaft extension with a flexible helical beam coupling. Due to the flexible coupling there exists the possibility of torsional vibrations appearing in the encoder readings that are not actually present in the compressor shaft. No specific accounting for torsional vibrations was taken in this study.

2.1 Parameter Identification
The methods developed below rely on many mechanical and electrical parameters, all of which should reasonably be known to the design engineers of the compressor manufacturer. However, the parameters used in this study were determined first hand due to the perceived difficulty of getting the manufacturer to divulge this information. The electrical parameters were determined with the use of the MATLAB system identification toolbox. A nonlinear "gray box" model of the induction motor was developed utilizing Park transformed voltage and encoder measured IAS as inputs and park transformed currents as outputs. A large scale iterative minimization procedure determined the initial state and motor model parameters concurrently to best reproduce the measured outputs. The choice to determine the motor model parameters in this fashion was done to most closely match their values to the application at hand, as opposed to fitting a steady state torque speed curve, a blocked rotor test, or a startup transient. The resulting parameters match well with simple checks by a resistance and inductance meter, as well as the results of traditional induction motor parameter estimation methods such as concurrently fitting a steady state torque speed curve and startup transient as in Shaw and Leeb (1999). The identified parameters form the basis of the industry standard "transformer equivalent" (t-model) or steady state circuit model of the induction motor.

2.2 Note on Data Gathering Procedure
The method relies on the assumption that the IAS of the compressor remains cyclic and repeatable over time scales of a few seconds. The best results are obtained from data sets gathered over tens of seconds, and the most stable period (lasting a few seconds or more) of motor current or power draw is identified and used as an input to the method. Since some parameters, such as resistance, vary strongly as a function of temperature, as well as the friction losses through the action of temperature dependent lubricant viscosity and distribution, the compressor was left to run to thermal steady state (usually an hour and a half) before the start of data collection.

3. INDUCTION MOTOR MODEL AND IAS RECOVERY

An induction motor can be modeled by the following system of non-linear differential equations expressed in the Park transform space:

$$\lambda'_s(t) = v_s(t) - R_s i_s(t) - j \omega_e \lambda_s(t) \tag{1}$$

$$\lambda'_r(t) = j\left(\frac{P}{2}\omega_r(t) - \omega_e\right)\lambda_r(t) - R_r i_r(t) \tag{2}$$

$$D i_s(t) = L_r \lambda_s - L_m \lambda_r \tag{3}$$

$$D i_r(t) = L_m \lambda_s - L_s \lambda_r \tag{4}$$

$$\omega'_r = \frac{3P}{2J}\left(\left(\Re i_r(t) \Im \lambda_r(t) - \Im i_r(t) \Re \lambda_r(t)\right) - \tau_l(t)\right) \tag{5}$$

The Park transform takes the three phase wall currents and voltages and transforms them to a pair of orthogonal space vectors (the D and Q axis) that rotate synchronously with the electrical supply frequency, ω_e. The Park transform is described in many sources (Park 1929). Its benefits include the expression of the simplified motor model equations (1)(2)(3)(4)(5).

3.1 Instantaneous Angular Speed Recovery

This system (1)(2)(3)(4)(5) is forced, where the forcing is provided by the stator voltage v_s and the load torque τ_l. The complete solution to the system consists of the stator current i_s, rotor current i_r, stator flux λ_s, rotor flux λ_r, and shaft angular speed ω_r (also referred to as the IAS). These quantities (excepting the IAS) are the complex phasors resulting from combining the D and Q axis components. In the application considered in this paper, only part of the forcing, v_s, is measured; the torque τ_l is not. This information alone would be insufficient to reconstruct the complete solution to the system. However, we are also provided with measured i_s, which allows the remainder of the solution to be determined; furthermore, the unknown forcing τ_l can also be determined.

Begin by noting that (1) is a linear first-order constant coefficient differential equation for $\lambda_s(t)$. This system has forcing function (6).

$$f(t) = v_s(t) - R_s i_s(t) \tag{6}$$

The solution to this differential equation consists of two parts: a particular solution (response to forcing) and a homogeneous part. First, let us focus on the particular solution. To avoid some of the inaccuracy that would result from a straightforward numerical derivative (for example, by approximating the derivative at each $f(t)$ by the secant line through the closest pair of samples), we instead note that both the forcing and response are periodic, band-limited, and finite energy. Consequently, all signals of interest admit a Fourier series description. Let $v_{s,k}$, $i_{s,k}$, f_k, and $\lambda_{s,k}$ denote the k-th Fourier series coefficient of v_s, i_s, f, and λ_s, respectively. Then clearly,

$$\lambda_{s,k} = \frac{f_k}{j(k\omega_0 + \omega_e)} \tag{7}$$

where ω_0 is the sampling frequency relative to the length of the data set in radians, and f_k is:

$$f_k = v_{s,k} - R_s i_{s,k} \tag{8}$$

The homogeneous solution to this equation consists of a single complex exponential of the form $A e^{j\omega_e t}$, for some complex A. To obtain the value of this A, one would need the initial condition of $\lambda_s(t)$. This is generally not easily obtainable. Fortunately, the homogeneous part has all of its energy at a single frequency, ω_e, which does not

interfere with any of the essential speed oscillation harmonics. Moreover, it is comparatively small. Thus it can be safely ignored. In the remainder of this section, the particular solution will be treated as the complete solution for λ_s .

One could immediately obtain an expression for the time domain waveform $\lambda_s(t)$ from the Fourier coefficients $\{\lambda_{s,k}\}_k$, but as our goal is to obtain $\omega_r(t)$, not $\lambda_s(t)$, it suffices to continue computing in the frequency domain until the final step. This has the advantage of avoiding the computational effort of computing an unnecessary reconstruction of a waveform from its frequency content, as well as any associated numerical error. It is important to note here that, while the forcing function f of this differential equation is different from the forcing of the actual system, which consists of only v_s and τ , the solution is still the actual λ_s because the forcing to the differential equation from i_s uses the true i_s of the actual system.

Next, we use (3) to obtain an equation for $\lambda_{r,k}$, the k-th Fourier series coefficients of $\lambda_r(t)$ in terms of known quantities. In particular,

$$\lambda_{r,k} = \frac{L_r \lambda_{s,k} - D i_{s,k}}{L_m} \tag{9}$$

Similarly, we use (4) to obtain

$$i_{r,k} = \frac{L_m \lambda_{s,k} - L_s \lambda_{s,k}}{D} \tag{10}$$

Lastly, we have

$$\omega_r(t) = \frac{2}{P} \left(\frac{a(t)}{j \lambda_r(t)} + \omega_e \right) \tag{11}$$

where the time-domain waveform $a(t)$ as Fourier series coefficients $\{a_k\}_k$ given by

$$a_k = \lambda_{r,k} + R_r i_{r,k} \tag{12}$$

It should be noted that, while this last equation does use the time domain waveforms $\lambda_r(t)$ and $a(t)$, it is only necessary to determine the values of these waveforms at the sampling times at which $\omega_r(t)$ is desired. In addition, knowledge of $\lambda_r(t)$ and $i_r(t)$ is sufficient to recover the torque generated by the induction motor $\tau_m(t)$ using equation (13). Plugging in $\lambda_r(t)$, $i_r(t)$, and $\omega_r(t)$ into equation (5) also allows one to solve for $\tau_l(t)$.

$$\tau_m(t) = \frac{3P}{2} \left(\Re i_r(t) \Im \lambda_r(t) - \Im i_r(t) \Re \lambda_r(t) \right) \tag{13}$$

3.2 Data Conditioning Procedures
The above scheme provides an efficient and reasonably accurate method of estimating $\omega_r(t)$ given only knowledge of $v_s(t)$ and $i_s(t)$. The implemented method includes several additional accuracy improvements which will now be discussed. The first accuracy improvement stems from the fact that $i_s(t)$ should only have content at the frequency corresponding to the line frequencies as well as at a discrete set of frequencies that are integer multiples of the shaft speed, assuming a reasonably healthy motor. Thus, we can filter out much of the measurement noise in $i_s(t)$ by throwing out all content that does not occur at one of the above frequencies. This was achieved by rotation domain averaging (refer to Stander and Heyns 2005), a technique that requires the average angular speed. However, the average angular speed is easily obtained from dominant spikes in the Park transformed current spectrum as shown in Figure 1. Measurement noise in $v_s(t)$ data is addressed by recognizing that it should not contain any information

from shaft speed harmonics and can therefore be taken as a constant value equal to its DC level over the time range of interest.
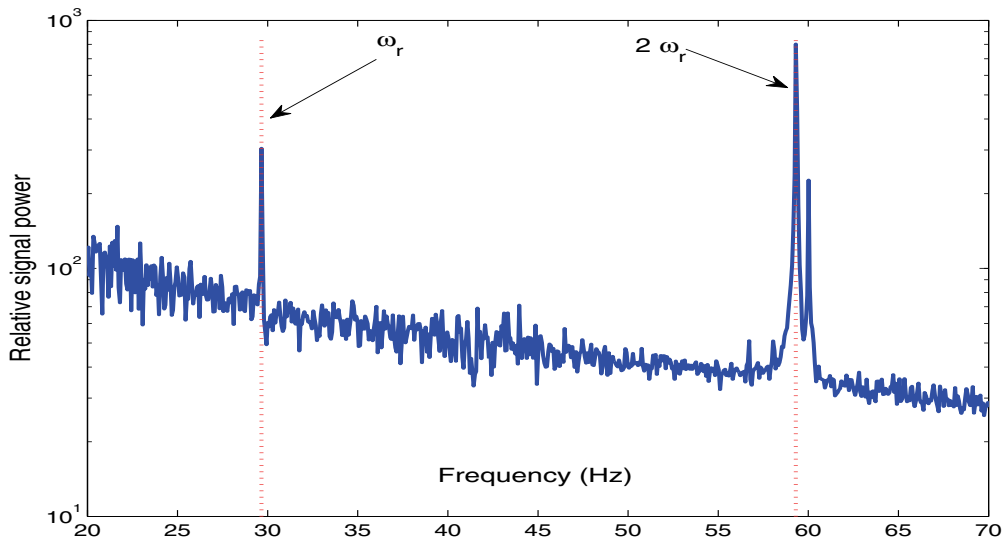

Figure 1: Dominant spikes at multiples of the average rotational speed in the frequency spectrum of D-axis stator current.

The second accuracy improvement uses the fact that the shaft speed $\omega_r(t)$ is purely real, while the IAS produced by the above method is not necessarily purely real, due to measurement inaccuracies in $v_s(t)$ and $i_s(t)$. To exploit the constraint that $\omega_r(t)$ should be purely real, we wish to project $i_s(t)$ and $v_s(t)$ onto a subspace for which the resulting $\omega_r(t)$ is purely real. This is done after the measurements are rotation domain averaged as described above. To do this, begin by noticing that, by the above calculations, there is a linear relation between the value of $a(t)$, at any particular t, and the Fourier coefficients $\{v_{s,k}\}_k$ and $\{i_{s,k}\}_k$. If we let $\bar{a}$ denote the vector of samples of $a(t)$, and $\bar{x}$ denote the vector whose first N elements are $\Re v_{s,k}$, next N elements are $\Re i_{s,k}$, next N elements are $j\Im v_{s,k}$, and final N elements are $j\Im i_{s,k}$, then we can write equation (14).

$$\bar{a} = A\bar{x} \tag{14}$$

where the matrix A is defined by applying (7)(9)(10)(12) and the Fourier synthesis equation. Using (11) we see that the constraint that $\omega_r(t)$ is purely real is equivalent to the constraint that each value of $a(t)$, after division by the corresponding value of $\lambda_r(t)$, is purely real. If we assume that the overall effect of measurement noise on the element-wise phase of $\lambda_r(t)$ (the phase of the complex number $\lambda_r(t)$ at any particular point in time t) is negligible, then we can use the values of $\lambda_r(t)$ obtained by the initial method to impose the constraint that $\omega_r(t)$ is purely real because only the phase of $\lambda_r(t)$ enters into the calculation, not the magnitude (again, in the element-wise sense). If we let R denote the matrix A after each row has been rotated by the phase of the corresponding $\lambda_r(t)$ (that is to say, each row is multiplied by the complex number $e^{-j\phi(t)}$, where $\phi(t)$ is the phase of λ_r evaluated at the time t corresponding to the row number). Then our constraint is simply that

$$\Re R\bar{x} = 0 \tag{15}$$

Due to the fact that the real and imaginary parts of $\bar{x}$ are conveniently separated (the first 2N elements are purely real and the last 2N elements are purely imaginary), then if we let R^* and $\bar{x}^*$ denote the (element-wise) conjugates of R and $\bar{x}$ respectively, we can write equation (16).

$$0 \;=\; \mathfrak{R}\, R\bar{x} \;=\; \frac{1}{2}\left(R\bar{x} + R^{*}\bar{x}^{*}\right) \;=\; C\bar{x} \tag{16}$$

where $C = R + Q$ and Q is the matrix formed from R^{*} by negating the last 2N columns (this follows from the fact that $\bar{x}^{*}$ is simply $\bar{x}$ with the last 2N entries negated, and we can distribute this negative sign into the matrix R^{*} that multiplies $\bar{x}^{*}$). Since (16) is simply the statement that $\bar{x} \in null(C)$, we can compute an orthogonal basis for the null space of C and project $\bar{x}$ onto that space. This produces a projected version of $i_{s,k}$ and $v_{s,k}$. These corrected data may then be used in the method above to produce an estimate of $\omega_{r}(t)$. Of course, this $\omega_{r}(t)$ is also not necessarily purely real, because we ignored the fact that the phase of $\lambda_{r}(t)$ is not exactly correct; however, this error is likely extremely small and so we can safely take $\mathfrak{R}\omega_{r}(t)$ as an accurate estimate of the IAS. Figure 2 shows the results of the IAS estimation method on a 15 second data set collected while the compressor was compressing from atmospheric pressure to atmospheric pressure through a small constriction on the discharge side. The rotational domain averaging technique and the projection procedure just described is used to produce the IAS estimate. For comparison the IAS as measured by the shaft encoder is also presented.
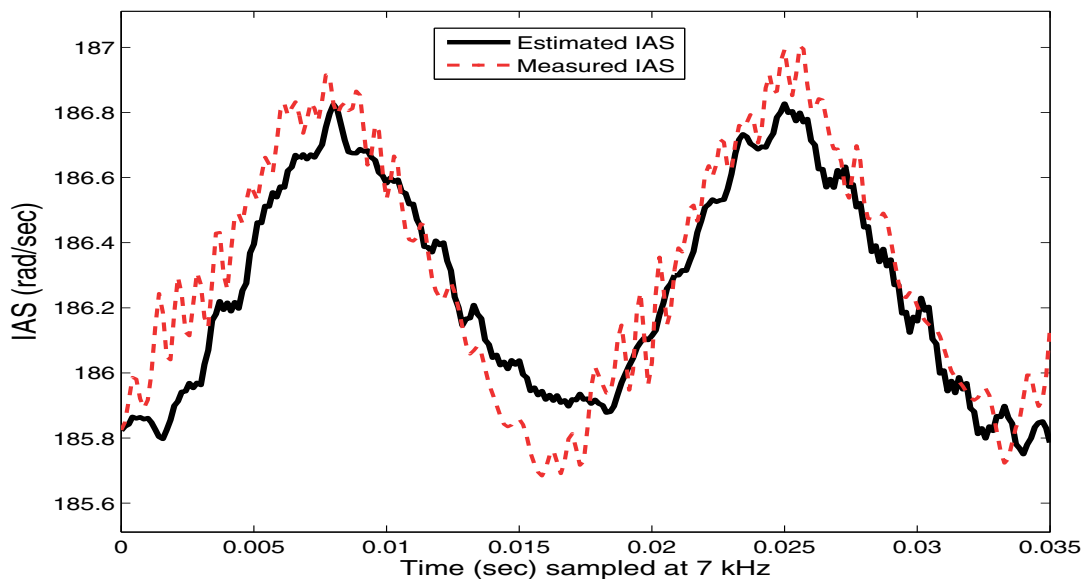

Figure 2: Typical IAS estimation results.

4. CONCLUSIONS AND FUTURE WORK

We have shown a method that is able to provide an estimate of the IAS speed of a compressor shaft using purely electrical measurements. The method succeeds where many speed-sensorless speed estimation methods would fail due in part to its incorporation of the full dynamic model of the induction motor. It is not limited by the assumption that the motor is in steady state or that the mechanical load dynamics are very much slower than the electrical dynamics. The IAS recovery method is still a prototype, but already the technique shows promise in providing additional information such as an accurate instantaneous induction motor torque measurement. Moreover, the method discussed is applicable to a wide range of repetitive motion induction motor driven machinery. By requiring only easily installed electrical sensors and a computation platform, the algorithm outlined in this paper lends itself to easy adoption via retrofit of existing systems or as a portable maintenance tool.

Preliminary attempts to use the estimated IAS and motor torque as inputs to an algorithm to recover compressor suction and discharge pressures are showing success. The ability to obtain the IAS, torque, and operating pressured of a reciprocating compressor without needing to install any mechanical sensors creates a promising and powerful new approach for fault detection and diagnosis of compressors and compressor systems.

NOMENCLATURE

L_m	Magnetizing Inductance	J	Rotational Inertia
L_{ls}	Stator leakage Inductance	P	Number of Induction Motor Poles
L_{lr}	Rotor leakage Inductance	D	Difference of L^2_m and $L_s L_r$
L_s	Sum of L_m and L_{ls}	j	Imaginary unit
L_r	Sum of L_m and L_{lr}		
$\Re$	Real part		**Subscripts**
$\Im$	Imaginary part	s	Stator quantities
R_r	Rotor resistance	r	Rotor quantities
R_s	Stator resistance	k	Frequency index

REFERENCES

Al-Qattan, M., Al-Juwayhel, F., Ball, A., Elhaj, M., Gu, F., 2009, Instantaneous Angular Speed and Power for the Diagnosis of Single-Stage, Double-Acting Reciprocating Compressor, *P. I. MECH. ENG. Part J Journal of Engineering Tribology*, vol. 223, no. 1, p. 95-114.

Angrilli, F., Basso, R., 1994, Monitoring and Diagnostics of Stresses in Reciprocating Machines, *Measurement,* vol. 12, no. 4, p. 345-356.

Citron, S., O'Higgins, J., Chen, L., 1989, Cylinder-by-Cylinder Engine Pressure and Pressure Torque Waveform Determination Utilizing Speed Fluctuations, *SAE Transactions,* paper no. 890486.

Elhaj, M., Gu, F., Ball, A., Albarbar, A., Al-Qattan, M., Naid, A., 2008, Numerical Simulation and Experimental Study of a Two-Stage Reciprocating Compressor for Condition Monitoring, *Mechanical Systems and Signal Processing*, vol. 22, no. 2, p. 374-389.

Gu, F., Jacob, P., Ball, A., 1999, Non-Parametric Models in the Monitoring of Engine Performance and Condition. Part 2: Non-Intrusive Estimation of Diesel Engine Cylinder Pressure and its use in Fault Detection, *P. I. MECH. ENG. Part D Journal of Automobile Engineering*, vol. 213, no. 2, p. 135-143.

Jacob, P., Gu, F., Ball, A., 1999, Non-Parametric Models in the Monitoring of Engine Performance and Condition. Part 1 : Modeling of Non-Linear Engine Processes, *P. I. MECH. ENG. Part D Journal of Automobile Engineering*, vol. 213, no. 1, p. 73-81.

Park, R., 1929, Two-Reaction Theory of Synchronous Machines: Generalized Method of Analysis, Part I, *Transactions of the AIEE*, vol. 48, p. 716-727.

Shaw, S., Leeb S., Norford, L., Cox, R., 2008, Nonintrusive Load Monitoring and Diagnostics in Power Systems, *IEEE TRANS. on Instrumentation and Measurement*, vol. 57, no. 7, p. 1445-1454.

Shaw, S., Leeb, S., 1999, Identification of Induction Motor Parameters from Transient Stator Current Measurements, *IEEE TRANS. on Industrial Electrons,* vol. 46, no. 1. p. 139-149.

Shi, K., Chan, T., Wong, Y., Ho, S., 2002, Speed Estimation of an Induction Motor Drive Using and Optimized Extended Kalman Filter, *IEEE TRANS. on Industrial Electrons,* vol. 49, no. 1, p. 124-133.

Stander, C., Heyns, P., 2005, Instantaneous Angular Speed Monitoring of Gearboxes Under Non-Cyclic Stationary Load Conditions, *Mechanical Systems and Signal Processing*, vol. 19, no. 4, p. 817-835 .

Kim, Y., Sul, S., Park, M., 1994, Speed Sensorless Vector Control of Induction Motor Using Extended Kalman Filter, *IEEE TRANS. on Industry Applications,* vol. 30, no. 5, p. 1225-1233.

ACKNOWLEDGEMENTS